ACS APPLIED MATERIALS & INTERFACES

Research Article

www.acsami.org

Electrochemical DNA Biosensor Based on a Tetrahedral Nanostructure Probe for the Detection of Avian Influenza A (H7N9) Virus

Shibiao Dong,[†,‡] Rongtao Zhao,[†] Jiangong Zhu,[∥] Xiao Lu,[†] Yang Li,[†] Shaofu Qiu,[†] Leili Jia,[†] Xiong Jiao,[‡] Shiping Song,[§] Chunhai Fan,[§] RongZhang Hao,*[,†] and HongBin Song*[,†]

[†]Institute for Disease Control and Prevention, Academy of Military Medical Sciences, Beijing 100071, China

[‡]Institute of Applied Mechanics and Biomedical Engineering, Taiyuan University of Technology, Taiyuan, Shanxi 030024, China

[§]Shanghai Institute of Applied Physics, Chinese Academy of Sciences, Shanghai 201800, China

[∥]Clinical Diagnostic Center, 302 Hospital of PLA, Beijing 100039, China

Supporting Information

ABSTRACT: A DNA tetrahedral nanostructure-based electrochemical biosensor was developed to detect avian influenza A (H7N9) virus through recognizing a fragment of the hemagglutinin gene sequence. The DNA tetrahedral probe was immobilized onto a gold electrode surface based on self-assembly between three thiolated nucleotide sequences and a longer nucleotide sequence containing complementary DNA to hybridize with the target single-stranded (ss)DNA. The captured target sequence was hybridized with a biotinylated-ssDNA oligonucleotide as a detection probe, and then avidin-horseradish peroxidase was introduced to produce an amperometric signal through the interaction with 3,3′,5,5′-tetramethylbenzidine substrate. The target ssDNA was obtained by asymmetric polymerase chain reaction (PCR) of the cDNA template, reversely transcribed from the viral lysate of influenza A (H7N9) virus in throat swabs. The results showed that this electrochemical biosensor could specifically recognize the target DNA fragment of influenza A (H7N9) virus from other types of influenza viruses, such as influenza A (H1N1) and (H3N2) viruses, and even from single-base mismatches of oligonucleotides. Its detection limit could reach a magnitude of 100 fM for target nucleotide sequences. Moreover, the cycle number of the asymmetric PCR could be reduced below three with the electrochemical biosensor still distinguishing the target sequence from the negative control. To the best of our knowledge, this is the first report of the detection of target DNA from clinical samples using a tetrahedral DNA probe functionalized electrochemical biosensor. It displays that the DNA tetrahedra has a great potential application as a probe of the electrochemical biosensor to detect avian influenza A (H7N9) virus and other pathogens at the gene level, which will potentially aid the prevention and control of the disease caused by such pathogens.

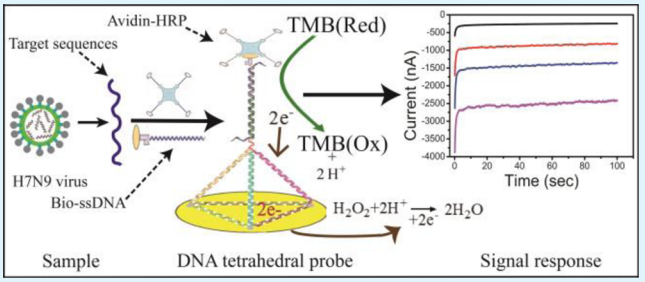

KEYWORDS: *electrochemical DNA biosensor, tetrahedral nanostructure probe, avian influenza A (H7N9) virus, asymmetric PCR, pathogen detection*

INTRODUCTION

Influenza virus can cause a highly infectious respiratory illness in humans, other mammals and birds. In the spring of 2013, a novel reassortant avian influenza A (H7N9) virus, causing human infections, was identified in China.[1] This new virus spread rapidly causing worldwide concern. Although the spread of this disease was largely controlled, it reemerged to cause sporadic infections in 2015.[2] The possibility that this avian influenza A (H7N9) virus could obtain high transmissibility through gene mutation leading to an epidemic cannot be excluded in the future. To prevent and control this disease, adequate detection methods for the rapid and accurate identification of A (H7N9) virus infected carriers are crucial. Traditional methods for the detection and identification of influenza A (H7N9) virus, such as polymerase chain reaction (PCR),[3] enzyme-linked immunosorbent assay[4] and serological methods[5] are usually laborious, time-consuming and expensive, and require specialized facilities and highly trained staff.[6] There is therefore increasing interest in the development of DNA electrochemical biosensors for the diagnosis of infectious pathogens because of their simplicity, low cost, high sensitivity, fast response time, easy operation and portability.[7,8] To date, DNA electrochemical biosensors have been applied for the detection of pathogens, such as *Aeromonas hydrophila*[9] and

Received: February 13, 2015
Accepted: April 6, 2015
Published: April 6, 2015

DOI: 10.1021/acsami.5b01438
ACS Appl. Mater. Interfaces 2015, 7, 8834−8842

Salmonella,[10] and for the detection of anthrax lethal factor.[11] They have also been applied for the detection of influenza viruses, including avian influenza A (H5N1) virus,[12] influenza viruses H5N2[13,14] and H7N9.[15] However, there have been no reports of the detection of natural nucleic acid from influenza A (H7N9) virus using DNA electrochemical biosensors.

High detection capabilities, that is, selectivity, specificity and stability, are a crucial feature of DNA biosensors.[16] The selectivity of nucleic acid hybridization assays primarily depend on the selection of the probe.[17] Therefore, several DNA probes such as single-stranded (ss) DNA, hairpin DNA,[18] peptide nucleic acid,[19] and locked nucleic acid,[20] have been developed for the construction of DNA biosensors. However, since most of these probes are attached to the electrode surface via a single-point-attachment, a passivation step with a blocker is still necessary to increase the heterogeneity of the biosensor surface.[21] Hence, it is vital to precisely control the surface density of the biosensor to obtain high reproducibility. DNA nanotechnology might potentially provide a new solution of these challenging problems. A DNA nanostructure, known as DNA tetrahedra, has been developed for molecular identification,[22−25] providing a convenient method of controlling the biomolecule-confined surface to increase molecular recognition at the biosensing interface.[21−23] When the three vertices of the tetrahedra were modified with thiol, it could be anchored onto the gold surface by strong Au−S chemical bonds, resulting in a 5000-fold greater affinity than single point-tethered oligonucleotides.[21,26] The fourth vertex at the top of the bound tetrahedra, appended with a pendant ssDNA probe, could further capture target DNA.[22] Importantly, the high mechanical rigidity of the tetrahedral nanostructural probe fixed it to the gold surface in an upright orientation, even in the absence of the "helper" molecule 6-mercapto-1-hexanol (MCH).[22] Some biosensors have been developed using DNA tetrahedra-structured probes to detect synthetic ssDNA samples with encouraging outcomes.[22,27] However, to date, this method has not been applied to the detection of clinical samples.

In recent years, conventional electrochemical detection methods have been able to sensitively detect DNA targets with high sequence specificity in pure DNA samples but the results do not meet clinical diagnostic requirements because of the high signal to background ratio resulting from the complexity of the sample.[28] Some DNA biosensors have also been developed for the detection of PCR products from practical samples.[29,30] However, similar problems were encountered, with low hybridization efficiency between target sequences and probes caused by background interference.[31] Ideally, for convenient detection, electrochemical biosensors for the detection of target DNA should be PCR-free or, at least, less dependent on PCR. PCR-free electrochemical biosensors mainly target the DNA analyte with high abundance. For target DNA of low abundance, although there have been reports on the detection of products by few PCR cycles (up to five cycles),[31] these reports are not based on DNA biosensor technology, but instead involved detection by quantitative real-time PCR.[31] In addition, to obtain ssDNA target sequences for biosensing detection, asymmetric PCR has been used,[31] which avoids the need for heat denaturation before hybridization with probes and reduces background interference.[31] The asymmetric PCR ssDNA products can then effectively hybridize with probes and many DNA biosensors can detect trace ssDNA sensitively.[32−34]

In this study, an electrochemical biosensor using DNA tetrahedral nanostructure as the probe was developed to detect the hemagglutinin (HA) gene of influenza A (H7N9) virus by amperometric measurements. In this system, three vertices of the tetrahedra modified with thiol were immobilized onto the gold surface and the fourth vertex appended with a pendant ssDNA as the coated probe. Then, a biotin-labeled (bio)-ssDNA was introduced as the detection probe to form a sandwich-type arrangement in the presence of target sequence. Avidin-horseradish peroxidase (HRP) was used as signal amplifier to transduce the DNA hybridization events to electrochemical signals by specific binding with the bio-ssDNA detection probes. To obtain ssDNA target sequences, asymmetric PCR was also used, employing A (H7N9) virus cDNA as template. The degree of dependence of electrochemical biosensing on PCR was also studied. To the best of our knowledge, this is the first report of the application of a tetrahedral DNA probe functionalized electrochemical biosensor for the detection of target DNA copied from clinical samples.

EXPERIMENTAL SECTION

Materials. All chemicals were obtained from commercial sources and used without further purification. Tris (2-carboxyehtyl) phosphine hydrochloride (TCEP), MCH and avidin-HRP were purchased from Sigma-Aldrich (St. Louis, MO, USA); avidin-HRP was diluted with 0.1% bovine serum albumin (Solarbio, Beijing, China). K_2HPO_4 was obtained from Strem Chemicals (Newburyport, MA, USA). TMB (enhanced K-blue substrate) was from Neogen (Pittsburgh, PA, U.S.A.). H_2SO_4 was from Merck (Darmstadt, Germany). KH_2PO_4 and KCl were from J&K Scientific (Beijing, China). All other reagents were purchased from Sinopharm Chemical Reagent Company (Shanghai, China). All solutions were prepared with double-distilled water (Milli-Q, 18 MΩ·cm resistivity from a Millipore system; Millipore, Bedford, MA, U.S.A.).

All of the DNA nucleotide sequences used as primers and probes in this work were supplied by Takara (Dalian, China), and their sequences are illustrated in Supporting Information Table S1, among which s1, s2, s3, and s4 were used to form DNA tetrahedral structured probes through self-assembling hybridization. Single primer H7-R, designed by DNAMAN v6 (Lynnon Biosoft, Los Angeles, CA, USA) according to the target sequence, was used to obtain ssDNA target sequences by asymmetric PCR. FluA-F30 and FluA-R264 were used in PCR for comparisons with established electrochemical biosensing methods.

Preparation of Samples. Influenza A (H7N9) RNA templates were viral lysates from throat swabs provided by the Chinese Center for Disease Control and Prevention (Beijing, China). Influenza A viruses, H3N2 and H1N1, from clinical samples were provided by the Beijing Center for Disease Prevention and Control (China), and routine laboratory methods were used for the propagation of influenza viruses. Viruses were cultured in Madin−Darby canine kidney (MDCK) cells supplemented with trypsin, as described by the World Health Organization guidelines.[35]

RNA from influenza A viruses, H3N2 and H1N1, was isolated after culturing with MDCK cells using the RNeasy Mini Kit according to the manufacturer's instructions (Qiagen, Hilden, Germany). cDNA was obtained using the Reverse Transcription System according to the manufacturer's instructions (Promega, Madison, WI, USA). To obtain ssDNA target sequences, asymmetric PCR was performed using the following reaction mixture: 25 μL Ex Taq Mix (Version 2.0, Takara), 1 μL cDNA, 0.5 μL H7-R, and 23.5 μL nuclease-free water, and the following cycling conditions: 1 min at 95 °C followed by 35 cycles of 95 °C for 30 s, 50 °C for 30 s, and 72 °C for 1 min; the reaction system was further incubated for 10 min at 72 °C to extend any incomplete products. The PCR products of the H7 sequences were confirmed by agarose gel electrophoresis and quantified by real-time

DOI: 10.1021/acsami.5b01438
ACS Appl. Mater. Interfaces 2015, 7, 8834−8842

PCR (the details are provided in Supporting Information). The primer sequences for real-time PCR (shown in Supporting Information Table S1) were based on the World Health Organization guidelines.[36]

Apparatus. All electrochemical measurements were performed using a CHI660D electrochemical workstation (CH Instrument Inc. 3700 Tennison Hill Drive Austin, TX 78738−5012 USA). The gold working electrode (CHI101), platinum wire counter electrode (CHI115) and Ag/AgCl reference electrode (CHI11) were also purchased from CH Instrument. The PCR thermal cycler (Veriti) was from Applied Biosystems (Foster City, CA, USA) and the iQ5 real-time PCR detection system was from Bio-Rad (Hercules, CA, USA).

Fabrication of the Electrochemical DNA Biosensor. The biosensor was fabricated through self-assembly via Au−S bonds between the thiolated tetrahedral structured DNA probes and the clean gold electrode, mainly according to previously reported methods.[37,38] The tetrahedral structured DNA probes were self-assembled by DNA hybridization between three thiolated DNA nucleotide sequences and a longer DNA nucleotide sequence containing the complementary sequence of the target sequence through a change in temperature. First, equimolar quantities of nucleotides (s1, s2, s3, s4) were mixed in TM buffer (10 mM Tris, 5 mM $MgCl_2$). Second, the mixture was heated to 95 °C for 2 min. Finally, the mixture was cooled at 4 °C for 30 s to form a DNA tetrahedral structure.[22,26,39] The successful assembly of the DNA tetrahedra was confirmed using polyacrylamide gel electrophoresis (PAGE), as described in the Supporting Information.

The gold electrode was polished with 1.0 μm alpha alumina powder on a nylon polishing pad for about 1 min, then with 0.3 μm alpha alumina powder on a nylon polishing pad for about 1.5 min, and finally with 0.05 μm gamma alumina powder on a microfiber polishing pad for about 2 min. The gold surface was rinsed with double distilled water after each polishing step. Next, the gold electrode was cleaned with piranha solution (7:3 ratio of H_2SO_4/30% H_2O_2 (v/v)) for 10 min to remove organic impurities and then rinsed with double-distilled water. (***Caution**: Piranha solution reacts violently with organic solvents and is a skin irritant, so extreme caution should be exercised when handling piranha solution.*) The cleaned gold electrode was further activated through an electrochemical cycle (about 15 cycles at 100 $mV \cdot s^{-1}$) from a potential of −0.3 to 1.55 V in 0.5 M H_2SO_4 solution until a stable gold oxidation peak at 1.06 V vs Ag/AgCl was observed. The bare gold electrode was reused as described above after each detection event.

The activated electrode was incubated with 1 μM of DNA tetrahedral structured probe in immobilization buffer (0.5 M KH_2PO_4, 0.5 M K_2HPO_4, 1 mM TCEP pH 7.4) at 4 °C overnight. The DNA tetrahedral structured probe modified electrode was then rinsed with double-distilled water to remove nonspecifically absorbed probes. Thus, the DNA nanostructure-based electrochemical biosensor was ready for the detection of target DNA sequences.

Electrochemical Measurements. During the process of electrochemical detection, synthetic targets (with concentrations of 0, 1 pM, 10 pM, 100 pM, 500 pM, 1 nM, 2.5 nM, 5 nM, 7.5 nM, 10 nM, 50 nM, and 100 nM) were mixed with 100 nM of bio-ssDNA detection probe solution at 37 °C for 30 min. Then, 4 μL of the mixture was incubated on the decorated gold electrode surface for 30 min at 37 °C to interact with the DNA tetrahedral structured probes. The mixture system was washed with PBS buffer followed by double-distilled water, and incubated with avidin-HRP (5 μg/mL) for 15 min at room temperature. After removing the remaining nonspecifically adsorbed HRP through washing with distilled water, amperometric detection was performed. Amperometric detection was performed at a fixed potential of 150 mV and a steady state was reached and recorded within 100 s, using TMB substrate as the electrolyte, under 300 $r \cdot min^{-1}$ agitation. A batch of parallel prepared electrodes modified with DNA tetrahedral probe were used to test their response to various concentration of targets, and this test was carried out 3 times to obtain error bars.

To evaluate the applicability of the fabricated biosensor to target sequences from clinical samples, asymmetric PCR ssDNA product targets were chosen at various concentrations (with dilution ratios of 1, 1/10, 1/100, 1/1000, 1/10000) and different cycle(s) (from 0 to 5) of asymmetric PCR ssDNA products, copied from cDNA of influenza A (H7N9) from swab samples. We also analyzed its detection capability for asymmetric PCR products compared with that for PCR-free products, which were obtained by heating the PCR-free samples at 95 °C for 5 min, then immediately chilling them on ice to obtain denatured ssDNA as described previously.[40]

To evaluate the specificity of the biosensor, 10 nM of various synthetic DNA sequences (complementary target, single-base mismatch mutant sequence, two-base mismatch, three-base mismatch and a random control sequence), and using three different asymmetric PCR products (cDNA from H7N9, H1N1, and H3N2 as templates) were tested.

The steps involved in fabricating the biosensor and detecting target DNA were also characterized by cyclic voltammetry (CV) and electrochemical impedance spectroscopy (EIS). CV, EIS, and amperometric detection (current versus time, $I-t$) were carried out on a CHI660D electrochemical workstation with a conventional three-electrode system composed of platinum wire as the auxiliary, Ag/AgCl electrode as the reference and a 2 mm diameter gold electrode as the working electrode. The CV curves were measured between −0.2 and 0.6 V in a solution of 1 mM $K_4Fe(CN)_6$, 1 mM $K_3Fe(CN)_6$, and 0.1 M KCl with a scan rate of 0.1 $V \cdot s^{-1}$. EIS measurements were conducted in the same solution under an AC amplitude of 0.01 V and a frequency ranging from 100 kHz to 0.01 Hz.

RESULTS AND DISCUSSION

Characterization of DNA Tetrahedra. The successful assembly of DNA tetrahedra was characterized by PAGE, as shown in Figure S1 in Supporting Information. The DNA tetrahedra was found to move more slowly than the ssDNA and two or three strands of DNA combinations, in accordance with previous reports.[22,39] The results indicated the successful assembly of the DNA tetrahedra nanostructure. PAGE analysis demonstrated that the yield of tetrahedra was more than 90%, as estimated by the TotalLab TL100 1D v. 2009 computer software package (Nonlinear Dynamics. Ltd.).

Electrochemical Characterization of the Biosensor Fabrication. The process of biosensor fabrication was characterized by the electrochemical methods of CV and EIS. Figure 1A shows the cyclic voltammogram behavior of the electroactive ion pair $[Fe(CN)_6]^{3-/4-}$ over the surface of the gold electrode before and after the process of modification of the DNA tetrahedral structured probes, the interaction with the target sequences and HRP labeling. For the bare gold electrode, there was a pair of redox peaks at 0.17 V (anodic, E_{pa}) and 0.24 V (cathodic, E_{pc}), and a peak potential difference ΔE_p of 0.07 V (a), which is attributed to the redox behavior of $[Fe(CN)_6]^{3-/4-}$.[41] After modification of the DNA tetrahedral structured probes through the thiol groups, the redox peak current decreased and the ΔEp increased significantly (b), which indicated that the binding of the thiol groups on the gold electrode surface hindered interfacial electron transfer between the gold surface and the bulk solution, and also suggested that the tetrahedral structured probes had been immobilized on the gold electrode surface.[37] However, after immersion in the target ssDNA/bio-ssDNA solution for 30 min, the CV curve presented almost no change compared with that of the modified DNA tetrahedral probes (c). This phenomenon might be attributed to the fact that the nanoscale interior pore space of the DNA tetrahedra makes the electrode surface accessible to the bulk solution by small molecules/ions such as $[Fe(CN)_6]^{3-/4-}$. This result was in accordance with reports that the DNA tetrahedra has mechanical rigidity and structural stability,[39] making the probes on top of the DNA tetrahedra

DOI: 10.1021/acsami.5b01438
ACS Appl. Mater. Interfaces 2015, 7, 8834−8842

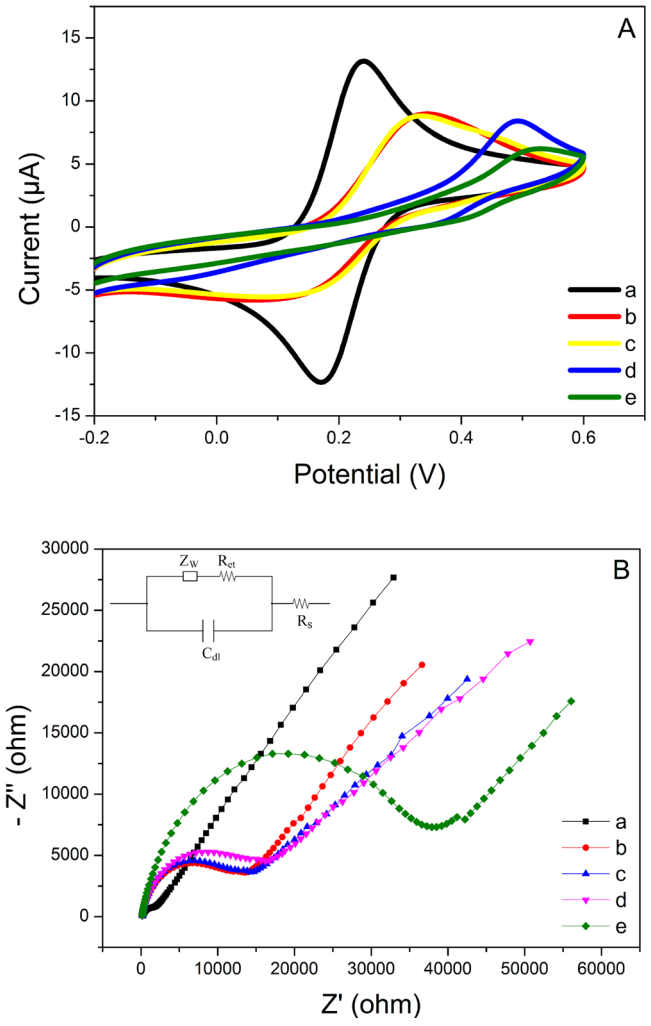

Figure 1. CV (A) and EIS (B) characteristics of the bare gold electrode (a), the modification with DNA tetrahedral probes (b), the hybridization with target ssDNA (10 nM)/bio-ssDNA (c), the binding with avidin-HRP (5 μg/mL) (e), and the binding with avidin-HRP directly after b but without c (d). The CV curves were measured between −0.2 and 0.6 V with a scan rate of 0.1 $V \cdot s^{-1}$, EIS measurements were conducted under an AC amplitude of 0.01 V and a frequency range from 100 kHz to 0.01 Hz. Work solution: 1 mM $K_4Fe(CN)_6$ + 1 mM $K_3Fe(CN)_6$ + 0.1 M KCl.

"stand up" in an orderly manner and a uniform orientation.[21,26] This structure may reduce the surface effects and place the probes in a solution-phase-like environment, enhancing biomolecular recognition and allowing enzyme amplification to increase the detection signal.[21,26] However, after incubation with avidin-HRP for 15 min, the redox peaks were significantly suppressed (e) compared with those for no target ssDNA/bio-ssDNA (d), indicating that the bulky streptavidin−HRP molecules adsorbed onto the electrode surface by bio-ssDNA/ssDNA blocked electron transfer and provided an effective barrier against electron transfer of the redox species in solution.

These findings were confirmed by EIS analysis. Figure 1B shows the EIS Nyquist plots after each electrode modification detailed in Figure 1A. As shown in Figure 1B (insert), the basic equivalent circuit model of the working electrode surface modified with an organic layer is made up of four parts, R_s, R_{et}, C_{dl}, and Z_W, representing the electrolyte resistance, electronic transfer resistance, double layer capacitance and the Warburg impedance, respectively. It is known that the impedance spectra includes a linear part at lower frequencies corresponding to diffusion and a semicircular portion at higher frequencies relating to the electron transfer-limited process, whose semicircular diameter was equal to electron-transfer resistance R_{et}.[37] The bare gold electrode exhibited an almost straight line (a, R_{et} = 1268 Ω), which was characteristic of the mass diffusion limiting step of the electron-transfer process. When the thiolated DNA tetrahedral structured probes were immobilized onto the electrode surface, a semicircular portion appeared in the higher frequency region, indicating an increase in R_{et} (b, R_{et} = 13110 Ω). This characteristic result was because the negatively charged phosphate backbone of the oligonucleotides produced an electrostatic repulsion force to $[Fe(CN)_6]^{3-/4-}$.[37] After the target ssDNA, hybridized with the introduced bio-ssDNA detection probes, the EIS Nyquist plots barely changed (c, R_{et} = 13840 Ω), which was consistent with the results obtained for CVs. When the avidin-HRP was introduced to bind to bio-ssDNA, a greater increase was observed in the semicircular portion (e, R_{et} = 37250 Ω), also in agreement with the results of CVs represented in Figure 1A.

Response of the Biosensor to Synthetic Target DNA. Figure 2A compares the signal obtained with the synthetic target DNA from the tetrahedral DNA probe functionalized biosensor with that obtained from the ssDNA probe biosensor. The results show that these two kinds of DNA probe biosensors have comparatively low background signals no matter through blocking with MCH or not. However, when detecting the targets, for instance under the same concentration of target synthetic DNA (1 nM), the tetrahedral DNA probe biosensor yielded 74.5% larger amperometric signal than the ssDNA probe biosensor without the blocking of MCH, showing significant statistical difference (P < 0.01 for t test). The blocking of MCH could increase the amperometric signal for these two kinds of biosensors, probably because of the orientation effect of MCH on the DNA probe on the electrode surface. However, the increase in the signal for the tetrahedral DNA probe functionalized biosensor (5.2%) was much lower than for the ssDNA probe biosensor (40%), which was perhaps due to the mechanical rigidity and structural stability of the tetrahedral nanostructure. The statistical analysis shows that the blocking of MCH could significantly increase the response signal of ssDNA probe functionalized biosensor (P < 0.01 for t test), but not for DNA tetrahedral probe functionalized biosensor (P = 0.6 for t test). These results indicate that the decoration of the tetrahedral nanostructured DNA probes on the electrode surface would not need further blocking with MCH to obtain a signal approximately equivalent to that with MCH blocking. Therefore, compared with the ssDNA probe, the tetrahedral DNA probe could not only increase the detection signal but could also reduce further decoration to facilitate the stability of the DNA biosensor.

To characterize the quantitative response capability of the fabricated biosensor to the target, synthetic oligonucleotides were used as targets in various concentrations to interact with the biosensor. Figure 2B (insert) presents the amperometric response value of the biosensor with target concentrations from 1 pM to 100 nM. The amperometric signals increased along with the concentration of target DNA. In general, the relationship between the signal and the logarithmic value of the target concentration was not linear, as usually reported.[42] However, when the curve was divided into two sections, from 1

DOI: 10.1021/acsami.5b01438
ACS Appl. Mater. Interfaces 2015, 7, 8834−8842

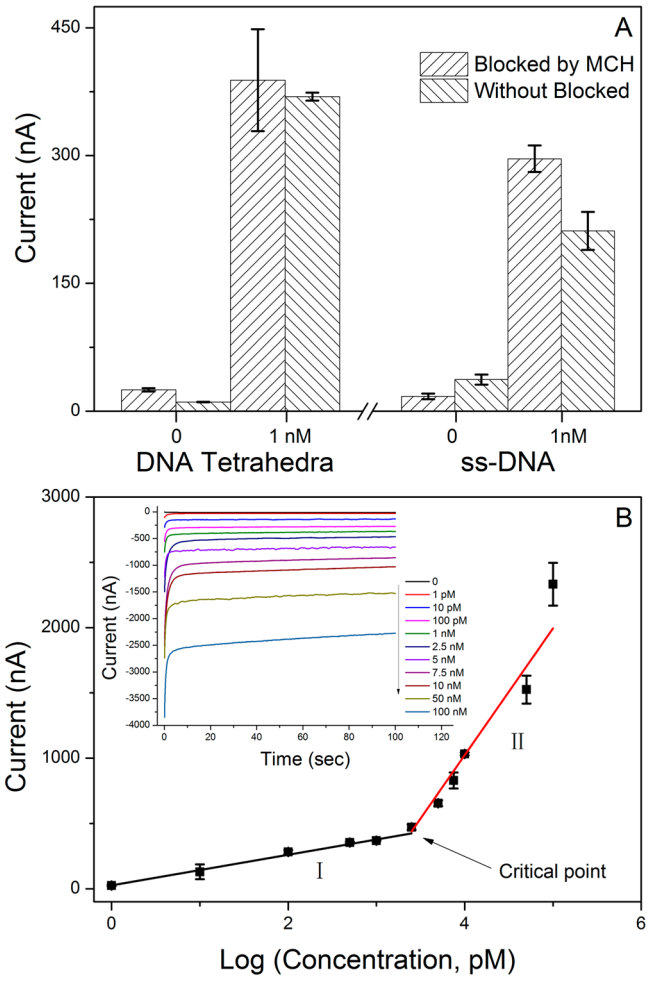

Figure 2. Amperometric response of the fabricated biosensor to synthetic target DNA. (A) Comparison between the signals for the biosensor of the tetrahedral DNA probe to 0 (blank) and 1 nM of synthetic target DNA and that for the ssDNA probe, with or without blocking by MCH. (B) The current variation of the tetrahedral DNA biosensor against the logarithmic value of the synthetic target DNA concentration from 1 pM to 100 nM. I and II show a linear relationship between the amperometric signal and the logarithmic value of the target concentration from 1 pM to 2.5 nM and from 2.5 nM to 100 nM, respectively (the R^2 values equal 0.995 and 0.966 for I and II, respectively). The inset shows the amperometric response against the target concentration. Error bar represents the relative standard deviation of three independent experiments.

pM to 2.5 nM (I on Figure 2B) and from 2.5 nM to 100 nM (II on Figure 2B) at the critical point 2.5 nM, the relationship between the amperometric signal and the logarithmic value of the target concentration was linear (the R^2 values were 0.995 and 0.966, respectively). The slope of the linearity curve increased with the target concentration. This result indicated that the hybridization of target DNA with the tetrahedral structured probes recognized the spatial conformation of DNA over the probes, which benefited the hybridization of subsequent DNA sequences to bind more avidin-HRP and significantly increase the signal.

To determine the detection limit of the biosensor for synthetic target DNA, the linearity plot of the amperometric signals against the target concentrations from 1 pM to 2.5 nM (I in Figure 2B) was used to estimate 3σ (where σ was the standard deviation of the signal for the blank solution). Thus, the detection limit was estimated to be 0.75 pM, slightly lower than that of a previous report (1 pM).[22]

Response of the Biosensor to Target DNA Sequences Derived from Clinical Samples Containing Influenza A (H7N9) Virus. Figure 3 shows the response of the biosensor to target DNA sequences derived from clinical samples containing influenza A (H7N9) virus. The amperometric signal of the biosensor to asymmetric PCR ssDNA products was larger than that for PCR-free samples at the same concentration (both 12 and 1.2 pM), except for the zero-sample (in the same hybridization reaction system but without samples), as displayed in Figure3A, which is due to less interference from the ssDNA target sequence from asymmetric PCR than that from the normal target DNA sequence without PCR. This result indicated that the application of asymmetric PCR can reduce the interference from complementary DNA sequences to the target DNA sequence, thereby increasing the detection signal. Furthermore, as shown in Figure 3B, the amperometric signals of the biosensor increased along with the concentration of asymmetric PCR products. The relationship between the signal and the logarithmic function of the concentration of asymmetric PCR ssDNA products was linear, indicating the quantitative detection ability of this biosensor for target DNA, as shown in Figure 3C. The detection limit of the biosensor for asymmetric PCR ssDNA products was determined to be 97 fM. These findings indicate that the biosensor could potentially be applied to the detection of clinical biological samples.

Specificity of the Biosensor for the Detection of the Influenza A (H7N9) HA Gene. The specificity of the biosensor was analyzed using artificial synthetic DNA and the products of asymmetric PCR from influenza A (H7N9) virus and negative control viruses including influenza A H3N2 and H1N1 viruses. Figure 4A shows the detection signal of the biosensor to synthetic DNA sequences at a concentration of 10 nM. The greatest amperometric response signal was observed with the complementary target sequence H7-T, this response signal was approximately an order of magnitude larger than that of the blank and random control DNA sequences. This result confirmed the high affinity of the biosensor to its complementary DNA target. As expected, significantly reduced amperometric signals were observed with DNA target sequences containing single-base, two-base or three-base mismatches. The response signals to synthetic nucleotide sequences indicated that the fabricated biosensor could discriminate different DNA sequences effectively, with excellent selectivity.

For the specific characterization of the fabricated biosensor with DNA sequences from clinical samples, three kinds of different asymmetric PCR products (diluted 1:100) were assayed: the ssDNA of influenza A viruses H7N9, H1N1, and H3N2, except for zero-samples. The concentration of the cDNA templates was checked after PCR by agarose gel electrophoresis, as shown in Figure 4B (insert). The results showed that the amperometric signal of the DNA biosensor for the target DNA from influenza A (H7N9) virus (labeled H7 in Figure. 4B) was greater than for influenza A H1N1 and H3N2 viruses (labeled H1 and H3 in Figure 4B), suggesting that the biosensor could specifically distinguish influenza A (H7N9) virus from other influenza A control viruses. This demonstrated the excellent specificity of the biosensor for the detection of the HA gene from influenza A (H7N9) virus.

Detection of Asymmetric PCR Products within Limited Cycles. To further test the ability of the biosensor

DOI: 10.1021/acsami.5b01438
ACS Appl. Mater. Interfaces 2015, 7, 8834−8842

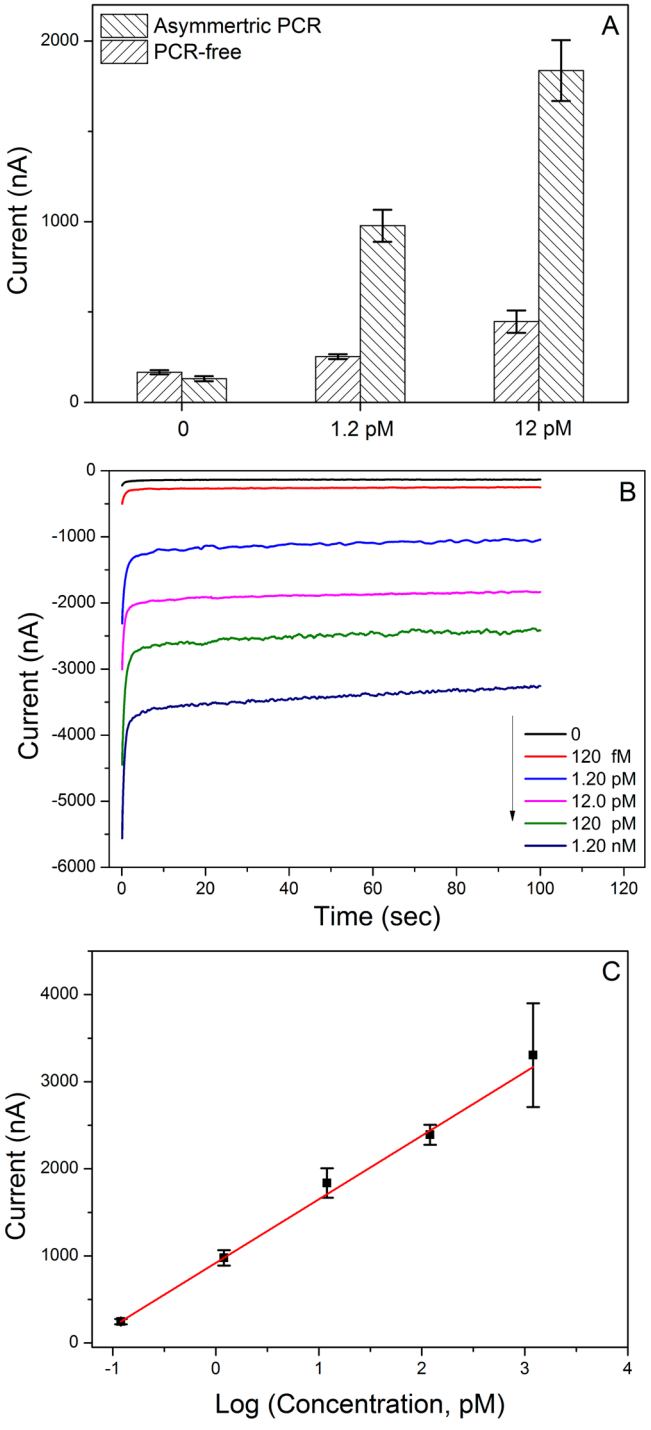

Figure 3. Amperometric response of the fabricated biosensor to various concentrations of target DNA derived from clinical throat-swab samples containing influenza A (H7N9) virus. (A) The amperometric response in the detection of asymmetric PCR ssDNA products and PCR-free samples (0, 1.2 pM and 12 pM). (B) The amperometric response with different concentrations of asymmetric PCR ssDNA products using influenza A (H7N9) cDNA as template (the electrophoretic profile of which is shown in Supporting Information Figure S2). (C) The linear relationship between the amperometric signal and the logarithmic function of the concentration of asymmetric PCR ssDNA products (the concentration of which was calculated according to the standard curve shown in Figure S3 in Supporting Information). Error bar represents relative standard deviation of three independent experiments.

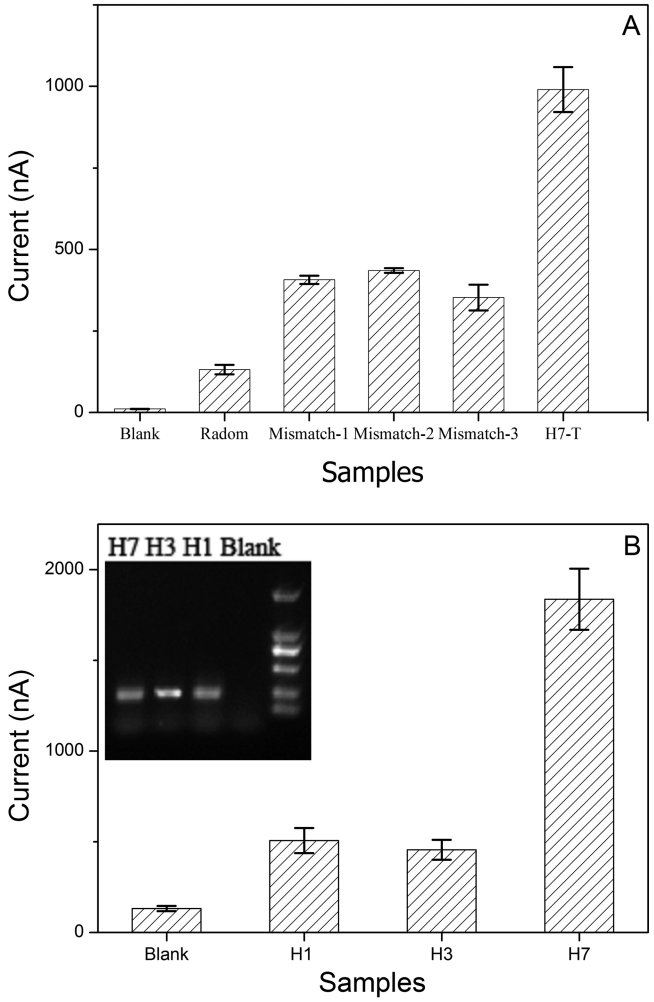

Figure 4. Specific response of the biosensor to the artificial synthetic DNA sequences and the asymmetric PCR products from influenza viruses. (A) Current signal response of the biosensor to synthetic complementary target sequences (H7-T) and control sequences with various numbers of mismatches or random control DNA sequences at a 10 nM concentration. (B) Current signal response of the biosensor to asymmetric PCR products using the cDNA templates of influenza A H7N9, H3N2, H1N1 viruses and zero-sample (labeled as H7, H3, H1, and blank respectively). The inset shows the electrophoretic separation of the PCR products amplified from the three cDNA templates described above using the Flu A primers (FluA-F30 and FluA-R264). Error bar represents the relative standard deviation of three independent experiments.

to detect clinical samples and potentially shorten the detection time, ssDNA asymmetric PCR products from 0 to 5 cycles were tested. As shown in Figure 5A, ssDNA products obtained from one cycle of asymmetric PCR could be distinguished by the DNA biosensor. This demonstrated the lack of dependence of the biosensor on PCR, a characteristic that would benefit the development of a PCR-free DNA biosensor for the detection of clinical nucleic acid samples with a greatly decreased processing time.

The specificity of this biosensor to ssDNA asymmetric PCR products, that had undergone three cycles of asymmetric PCR, were also evaluated with influenza A H7N9, H1N1 and H3N2 cDNA as templates, respectively. As shown in Figure 5B, the biosensor also displayed excellent sensitivity and specificity for the detection of three-cycle ssDNA asymmetric PCR products

DOI: 10.1021/acsami.5b01438
ACS Appl. Mater. Interfaces 2015, 7, 8834−8842

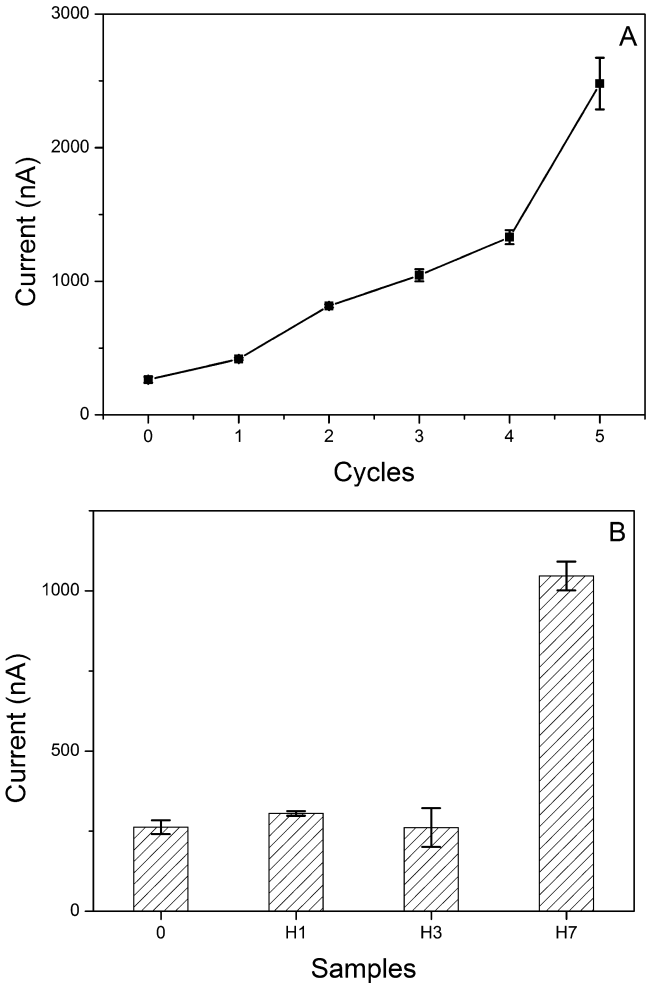

Figure 5. Response of the biosensor to the asymmetric PCR products amplified with a limited number of cycles. (A) The amperometric response to ssDNA products of asymmetric PCR comprising 0–5 cycles. (B) Current signal response to three cycles of asymmetric PCR from the templates: influenza A H7N9, H1N1, and H3N2 viruses. 0 represents the cDNA of the influenza A H7N9 HA gene without PCR and denaturation. Error bar represents the relative standard deviation of three independent experiments.

of the influenza A (H7N9) HA gene. The development of this tetrahedral DNA probe functionalized biosensor is a significant advance in the development of a PCR-free electrochemical biosensor to greatly reduce the time of sample pretreatment for on-site detection of influenza A (H7N9) virus. This biosensor may be an important tool in the process of preventing and controlling the disease caused by avian influenza A (H7N9) virus.

CONCLUSION

The tetrahedral structured DNA was used as the probe of a DNA electrochemical biosensor to detect the avian influenza A (H7N9) virus by amperometric measurements. The successful assembly of the DNA tetrahedral structure and its immobilization on a gold electrode surface was characterized by PAGE, CV, or EIS. Our findings demonstrated that the using of DNA tetrahedra as probe can improve the detection performance of electrochemical biosensor compared with ssDNA probe biosensors. This newly developed biosensor could be used for the detection of target DNA derived from clinical throat-swab samples containing influenza A (H7N9) virus. The detection sensitivity of the biosensor could reach 100 fM for target nucleotide sequences through the combined use of the DNA tetrahedral structure as probe and avidin-HRP as the signal amplifier. The selectivity experiments showed that this electrochemical biosensor could specifically recognize target DNA of influenza A (H7N9) virus from other types of influenza A viruses (H1N1 and H3N2), and even from single-base mismatch oligonucleotides. The dependence of the biosensor on PCR was also tested, and the results showed that the biosensor was able to sensitively and specifically detect asymmetric PCR ssDNA products of trace cDNA of the influenza A (H7N9) HA gene after only three cycles of PCR. This finding is promising with regard to the ultimate aim of developing a PCR-free DNA biosensor for the detection of nucleic acid samples on site, shortening sample processing time. It displays that the DNA tetrahedra has a great potential application as a probe of the electrochemical biosensor to detect avian influenza A (H7N9) virus and other pathogens at the gene level, which will potentially aid the prevention and control of the disease caused by such pathogens.

ASSOCIATED CONTENT

Supporting Information

Detailed methodology, three supplementary figures, a supplementary table, and formulas used in calculations. This material is available free of charge via the Internet at http://pubs.acs.org.

AUTHOR INFORMATION

Corresponding Authors

*Tel: +86 10 66948475. Fax: +86 10 66948475. E-mail: hrongzhang@163.com

*E-mail: hongbinsong@263.net.

Author Contributions

S.D., R.Z., and J.Z. contributed equally to this work. Academy of Military Medical Sciences and Taiyuan University of Technology contributed equally to this paper.

Notes

The authors declare no competing financial interest.

ACKNOWLEDGMENTS

This work was funded by the National High Technology Research and Development Program of China (No. 2015AA020929), Beijing Nova Program (No. Z141107001814071), the National Natural Science Foundation of China (No. 21105122), the Mega-projects of Science and Technology Research (No. 2012ZX10004801), and Beijing Natural Science Foundation (No. 7132164).

REFERENCES

(1) Gao, R. B.; Cao, B.; Hu, Y. W.; Feng, Z. J.; Wang, D. Y.; Hu, W. F.; Chen, J.; Jie, Z. J.; Qiu, H. B.; Xu, K.; Xu, X. W.; Lu, H. Z.; Zhu, W. F.; Gao, Z. C.; Xiang, N. J.; Shen, Y. Z.; He, Z. B.; Gu, Y.; Zhang, Z. Y.; Yang, Y.; Zhao, X.; Zhou, L.; Li, X. D.; Zou, S. M.; Zhang, Y.; Li, X. Y.; Yang, L.; Guo, J. F.; Dong, J.; Li, Q.; Dong, L. B.; Zhu, Y.; Bai, T.; Wang, S. W.; Hao, P.; Yang, W. Z.; Zhang, Y. P.; Han, J.; Yu, H. J.; Li, D. X.; Gao, G. F.; Wu, G. Z.; Wang, Y.; Yuan, Z. H.; Shu, Y. L. Human Infection with a Novel Avian-Origin Influenza A (H7N9) Virus. *N. Engl. J. Med.* **2013**, *368*, 1888–1897.

(2) World Health Organization. http://www.who.int/csr/don/11-march-2015-avian-influenza-china/en/ (accessed March 11, 2015).

(3) Kalthoff, D.; Bogs, J.; Harder, T.; Grund, C.; Pohlmann, A.; Beer, M.; Hoffmann, B. Nucleic Acid-based Detection of Influenza A Virus

DOI: 10.1021/acsami.5b01438
ACS Appl. Mater. Interfaces 2015, 7, 8834–8842

Subtypes H7 and N9 with a Special Emphasis on the Avian H7N9 Virus. *Eurosurveillance* **2014**, *19*, 30−42.
(4) Kang, K.; Chen, L.; Zhao, X.; Qin, C.; Zhan, Z.; Wang, J.; Li, W.; Dzakah, E. E.; Huang, W.; Shu, Y.; Jiang, T.; Cao, W.; Xie, M.; Luo, X.; Tang, S. Development of Rapid Rmmunochromatographic Test for Hemagglutinin Antigen of H7 Subtype in Patients Infected with Novel Avian Influenza A (H7N9) Virus. *PloS One* **2014**, *9*, No. e92306.
(5) Dong, L. B.; Bo, H.; Bai, T.; Gao, R. B.; Dong, J.; Zhang, Y.; Guo, J. F.; Zou, S. M.; Zhou, J. F.; Zhu, Y.; Xin, L.; Li, X. D.; Xu, C. L.; Wang, D. Y.; Shu, Y. L. A Combination of Serological Assays to Detect Human Antibodies to the Avian Influenza A H7N9 Virus. *PloS One* **2014**, *9*, No. e95612.
(6) Amano, Y.; Cheng, Q. Detection of Influenza Virus: Traditional Approaches and Development of Biosensors. *Anal. Bioanal. Chem.* **2005**, *381*, 156−164.
(7) Kimmel, D. W.; LeBlanc, G.; Meschievitz, M. E.; Cliffel, D. E. Electrochemical Sensors and Biosensors. *Anal. Chem.* **2012**, *84*, 685−707.
(8) Kumar, H.; Rani, R. Development of Biosensors for the Detection of Biological Warfare Agents: Its Issues and Challenges. *Sci. Prog.* **2013**, *96*, 294−308.
(9) Ligaj, M.; Tichoniuk, M.; Gwiazdowska, D.; Filipiak, M. Electrochemical DNA Biosensor for the Detection of Pathogenic Bacteria *Aeromonas Hydrophila*. *Electrochim. Acta* **2014**, *128*, 67−74.
(10) Garcia, T.; Revenga-Parraa, M.; Anorga, L.; Arana, S.; Pariente, F.; Lorenzo, E. Disposable DNA Biosensor Based on Thin-film Gold Electrodes for Selective Salmonella Detection. *Sens. Actuators, B* **2012**, *161*, 1030−1037.
(11) Wang, L.; Han, Y.; Zhou, S.; Wang, G.; Guan, X. Nanopore Biosensor for Label-free and Real-time Detection of Anthrax Lethal Factor. *ACS Appl. Mater. interfaces* **2014**, *6*, 7334−7339.
(12) Grabowska, I.; Stachyra, A.; Gora-Sochacka, A.; Sirko, A.; Olejniczak, A. B.; Lesnikowski, Z. J.; Radecki, J.; Radecka, H. DNA Probe Modified with 3-iron bis(dicarbollide) for Electrochemical Determination of DNA Sequence of Avian Influenza Virus H5N1. *Biosens. Bioelectron.* **2014**, *51*, 170−176.
(13) Lai, Y. H.; Lee, C. C.; King, C. C.; Chuang, M. C.; Ho, J. A. A. Exploitation of Stem-loop DNA as a Dual-input Gene Sensing Platform: Extension to Subtyping of Influenza A Viruses. *Chem. Sci.* **2014**, *5*, 4082−4090.
(14) Grabowska, I.; Malecka, K.; Stachyra, A.; Gora-Sochacka, A.; Sirko, A.; Zagorski-Ostoja, W.; Radecka, H.; Radecki, J. Single Electrode Genosensor for Simultaneous Determination of Sequences Encoding Hemagglutinin and Neuraminidase of Avian Influenza Virus Type H5N1. *Anal. Chem.* **2013**, *85*, 10167−10173.
(15) Yu, Y.; Chen, Z.; Jian, W.; Sun, D.; Zhang, B.; Li, X.; Yao, M. Ultrasensitive Electrochemical Detection of Avian Influenza A (H7N9) Virus DNA Based on Isothermal Exponential Amplification Coupled with Hybridization Chain Reaction of DNAzyme Nanowires. *Biosens. Bioelectron.* **2015**, *64*, 566−571.
(16) Laschi, S.; Palchetti, I.; Marrazza, G.; Mascini, M. Enzyme-amplified Electrochemical Hybridization Assay Based on PNA, LNA and DNA Probe-modified Micro-magnetic Beads. *Bioelectrochemistry* **2009**, *76*, 214−220.
(17) Wang, J. DNA Biosensors Based on Peptide Nucleic Acid (PNA) Recognition Layers. A Review. *Biosens. Bioelectron.* **1998**, *13*, 757−762.
(18) Lin, L. Q.; Weng, S. H.; Zhao, C. F.; Liu, Q. C.; Liu, A. L.; Lin, X. H. Hairpin LNA Biosensor with Enzyme Tagged AuNPs as Tracer for Amperometric Detection of K-ras Mutation Gene. *Electrochim. Acta* **2013**, *108*, 808−813.
(19) Prabhakar, N.; Arora, K.; Singh, H.; Malhotra, B. D. Polyaniline Based Nucleic Acid Sensor. *J. Phys. Chem. B* **2008**, *112*, 4808−4816.
(20) Meng, X. M.; Xu, M. R.; Zhu, J. Y.; Yin, H. S.; Ai, S. Y. Fabrication of DNA Electrochemical Biosensor Based on Gold Nanoparticles, Locked Nucleic Acid Modified Hairpin DNA and Enzymatic Signal Amplification. *Electrochim. Acta* **2012**, *71*, 233−238.
(21) Pei, H.; Zuo, X. L.; Zhu, D.; Huang, Q.; Fan, C. H. Functional DNA Nanostructures for Theranostic Applications. *Acc. Chem. Res.* **2014**, *47*, 550−559.
(22) Pei, H.; Lu, N.; Wen, Y. L.; Song, S. P.; Liu, Y.; Yan, H.; Fan, C. H. A DNA Nanostructure-Based Biomolecular Probe Carrier Platform for Electrochemical Biosensing. *Adv. Mater.* **2010**, *22*, 4754−4758.
(23) Li, Z.; Zhao, B.; Wang, D.; Wen, Y.; Liu, G.; Dong, H.; Song, S.; Fan, C. DNA Nanostructure-Based Universal Microarray Platform for High-Efficiency Multiplex Bioanalysis in Biofluids. *ACS Appl. Mater. interfaces* **2014**, *6*, 17944−17953.
(24) Zhang, M.; Jiang, X. Q.; Le, H. N.; Wang, P.; Ye, B. C. Dip-and-Read Method for Label-Free Renewable Sensing Enhanced using Complex DNA Structures. *ACS Appl. Mater. interfaces* **2013**, *5*, 473−478.
(25) Abi, A.; Lin, M.; Pei, H.; Fan, C.; Ferapontova, E. E.; Zuo, X. Electrochemical Switching with 3D DNA Tetrahedral Nanostructures Self-assembled at Gold Electrodes. *ACS Appl. Mater. interfaces* **2014**, *6*, 8928−8931.
(26) Schlapak, R.; Danzberger, J.; Armitage, D.; Morgan, D.; Ebner, A.; Hinterdorfer, P.; Pollheimer, P.; Gruber, H. J.; Schaffler, F.; Howorka, S. Nanoscale DNA Tetrahedra Improve Biomolecular Recognition on Patterned Surfaces. *Small* **2012**, *8*, 89−97.
(27) Lin, M. H.; Wen, Y. L.; Li, L. Y.; Pei, H.; Liu, G.; Song, H. Y.; Zuo, X. L.; Fan, C. H.; Huang, Q. Target-responsive, DNA Nanostructure-based E-DNA Sensor for MicroRNA Analysis. *Anal. Chem.* **2014**, *86*, 2285−2288.
(28) Lin, L.; Liu, Q.; Wang, L.; Liu, A.; Weng, S.; Lei, Y.; Chen, W.; Lin, X.; Chen, Y. Enzyme-Amplified Electrochemical Biosensor for Detection of PML-RARalpha Fusion Gene Based on Hairpin LNA Probe. *Biosens. Bioelectron.* **2011**, *28*, 277−283.
(29) Liu, G.; Wan, Y.; Gau, V.; Zhang, J.; Wang, L. H.; Song, S. P.; Fan, C. H. An Enzyme-Based E-DNA Sensor for Sequence-specific Detection of Femtomolar DNA Targets. *J. Am. Chem. Soc.* **2008**, *130*, 6820−6825.
(30) Pohlmann, C.; Wang, Y. R.; Humenik, M.; Heidenreich, B.; Gareis, M.; Sprinzl, M. Rapid, Specific and Sensitive Electrochemical Detection of Foodborne Bacteria. *Biosens. Bioelectron.* **2009**, *24*, 2766−2771.
(31) Tosar, J. P.; Branas, G.; Laiz, J. Electrochemical DNA Hybridization Sensors Applied to Real and Complex Biological Samples. *Biosens. Bioelectron.* **2010**, *26*, 1205−1217.
(32) Duwensee, H.; Mix, M.; Stubbe, M.; Gimsa, J.; Adler, M.; Flechsig, G. U. Electrochemical Product Detection of an Asymmetric Convective Polymerase Chain Reaction. *Biosens. Bioelectron.* **2009**, *25*, 400−405.
(33) Loaiza, O. A.; Campuzano, S.; Pedrero, M.; Garcia, P.; Pingarron, J. M. Ultrasensitive Detection of Coliforms by Means of Direct Asymmetric PCR Combined with Disposable Magnetic Amperometric Genosensors. *Analyst* **2009**, *134*, 34−37.
(34) Wu, G.; Kang, H. B.; Zhang, X. Y.; Shao, H. B.; Chu, L. Y.; Ruan, C. J. A Critical Review on the Bio-removal of Hazardous Heavy Metals from Contaminated Soils: Issues, Progress, Eco-environmental Concerns and Ppportunities. *J. Hazard. Mater.* **2010**, *174*, 1−8.
(35) *Manual for the Laboratory Diagnosis and Virological Surveillance of Influenza*; World Health Organization: Geneva, Switzerland, 2011.
(36) World Health Organization. http://www.who.int/influenza/gisrs_laboratory/cnic_realtime_rt_pcr_protocol_a_h7n9.pdf?ua=1 (accessed April 8, 2013).
(37) McEwen, G. D.; Chen, F.; Zhou, A. H. Immobilization, Hybridization, and Oxidation of Synthetic DNA on Gold Surface: Electron Transfer Investigated by Electrochemistry and Scanning Tunneling Microscopy. *Anal. Chim. Acta* **2009**, *643*, 26−37.
(38) Steel, A. B.; Herne, T. M.; Tarlov, M. J. Electrochemical Quantitation of DNA Immobilized on Gold. *Anal. Chem.* **1998**, *70*, 4670−4677.
(39) Goodman, R. P.; Schaap, I. A. T.; Tardin, C. F.; Erben, C. M.; Berry, R. M.; Schmidt, C. F.; Turberfield, A. J. Rapid Chiral Assembly of Rigid DNA Building Blocks for Molecular Nanofabrication. *Science* **2005**, *310*, 1661−1665.

DOI: 10.1021/acsami.5b01438
ACS Appl. Mater. Interfaces 2015, 7, 8834−8842

(40) Singh, R.; Sumana, G.; Verma, R.; Sood, S.; Pandey, M. K.; Gupta, R. K.; Malhotra, B. D. DNA Biosensor for Detection of Neisseria Gonorrhoeae Causing Sexually Transmitted Disease. *J. Biotechnol.* **2010**, *150*, 357−365.
(41) Mashhadizadeh, M. H.; Talemi, R. P. A New Methodology for Electrostatic Immobilization of a Non-labeled Single Strand DNA onto a Self-assembled Siazonium Modified Gold Electrode and Detection of its Hybridization by Differential Pulse Voltammetry. *Talanta* **2013**, *103*, 344−348.
(42) Wang, Z. J.; Yang, Y. H.; Leng, K. L.; Li, J. S.; Zheng, F.; Shen, G. L.; Yu, R. Q. A Sequence-Selective Electrochemical DNA Biosensor Based on HRP-labeled Probe for Colorectal Cancer DNA Detection. *Anal. Lett.* **2008**, *41*, 24−35.

DOI: 10.1021/acsami.5b01438
ACS Appl. Mater. Interfaces 2015, 7, 8834−8842